

## Forest mapping with ERS SAR interferometry

Tazio Strozzi

Gamma Remote Sensing, Thunstrasse 130  
CH-3074 Muri b. Bern, Switzerland  
Tel: +41(0)31-951.70.05, Fax: +41(0)31-951.70.08  
email: gamma\_rs@pingnet.ch

Urs Wegmüller

Gamma Remote Sensing, Thunstrasse 130  
CH-3074 Muri b. Bern, Switzerland  
Tel: +41(0)31-951.70.05, Fax: +41(0)31-951.70.08  
email: gamma\_rs@pingnet.ch

### Abstract

**The geometric information contained in the interferometric phase and the potential of the interferometric correlation and of the two backscatter intensities of an interferometric pair for the classification of different surface types were combined in order to generate a forest map for a part of Switzerland. Forest was mapped based on its low interferometric correlation, low backscatter change between the two images of the interferometric pair, and backscattering intensities around -10 dB. The described approach was applied to several ERS-1/2 Tandem pairs allowing to discuss the dependence of the result on system and scene parameters, including seasonal and meteorological effects. As a result of the short one day acquisition interval (as compared to the 3 and more days with ERS-1, only) less confusion occurred between forest stands, on one side, and vegetation on agricultural fields or low correlation by farming activities, on the other side. This makes the approach with Tandem data more robust for application during spring, summer and fall. The resulting landuse maps were transformed into orthonormal coordinates using the estimated topographic heights and validated with data of the Swiss Federal Statistical Institute.**

**The potential of SAR interferometry for forest type discrimination was also investigated. For known forest stands the interferometric correlation was related to the forest type. A reliable separation for deciduous, mixed, and coniferous forest stands was possible only with winter Tandem pairs.**

*Keywords: SAR, SAR interferometry, ERS, forest mapping*

### Introduction

Based on ERS-1 data acquired during 3-day repeat orbits a good potential of repeat-pass SAR interferometry for land applications such as landuse classification, forest mapping, and change detection was identified (Wegmüller et al., 1995a, 1995b, and 1997a). It was found that the interferometric correlation is not just a measure of the phase noise of the interferogram but a valuable source of information on scene properties. With the ERS-1/2 Tandem mission repeat-pass SAR data useful for interferometric analysis became widely available (Wegmüller and Werner, 1996). The 1-day acquisition time interval and the precise orbit control which allowed to almost permanently obtain short interferometric baselines for Tandem pairs resulted in data ideal for interferometry. In addition the 35-day repeat-orbits of the two satellites allowed to achieve nearly global coverage. With the available data interferometric techniques can now be extensively applied.

In this paper it will be shown that Tandem data are very useful for forest mapping of a part of Switzerland. The classification algorithm is based on the interferometric correlation, the two backscatter intensities of an interferometric pair, and the texture of the backscatter image. The dependence of the resulting maps on system and scene parameters, including seasonal and meteorological effects, will be discussed. The maps will be validated against available landuse inventory. Finally, the potential of SAR interferometry for forest type discrimination will be investigated.

### Interferometric Data Processing

For the analysis of the interferometric signatures and for the forest mapping, the ERS SAR data were processed using Gamma's SAR and interferometric processing softwares (Wegmüller and Werner, 1997b). ERS SAR raw products were used. This has the advantage that data for full ERS frames are available. Another advantage is that by carrying out the SAR processing we have full control over this step. Data were processed to full resolution. The processing included radiometric calibration for the antenna gain and slant range distance. The resulting single look complex (SLC) images look well focused and allowed to produce interferograms of high quality.

Interferometric processing of complex SAR data combines two SLC images into an interferogram. In a first step the two images are co-registered at sub-pixel accuracy. In the same step common band filtering of the azimuth and range spectra is applied in order to include only those parts of the spectra which are common to the two images, and thereby optimizing the interferometric correlation and minimizing the effects of the baseline geometry on the interferometric correlation. Then the two images are cross correlated, i.e. the normalized complex interferogram is computed. The azimuth and range phase trends expected for a flat Earth are then removed from the interferogram. From this "flattened" interferogram and the two registered intensity images, the multi-look interferometric correlation and backscatter intensities are estimated. In further steps the topographic height is computed. Knowing the topographic heights allows to transform the images from SAR coordinates (slant range, azimuth) to orthonormal map coordinates. In addition, the true pixel size can be estimated and used to correct the normalization of the backscattering intensities and to avoid errors in the estimation of the interferometric correlation due to sloped terrain.

One of the main problems encountered when using SAR data for classification purposes is the strong signal noise or speckle of unfiltered SAR images. One way to solve this problem is to carry out a segmentation before estimating average signatures for the image segments. Here we did not follow this approach. The presented landuse classification scheme is based on the normalized interferogram and the two backscatter intensity images of the interferometric image pair. In a first step these data are used to estimate (1) the interferometric correlation, (2) the average backscatter intensity, (3) the backscatter intensity change, and (4) the texture of one of the backscatter images. For a wide applicability, the classification is made on a per pixel level. In order to obtain reliable values at the per pixel level appropriate estimators and filtering are required. A detailed discussion on the estimation of the parameters used for the classification is given in Wegmüller and Werner (1996). Here the main features regarding the interferometric correlation, the average backscatter intensity, the backscatter intensity change, and the texture are summarized.

The interferometric correlation is a measure of the phase noise of the interferogram. It depends on sensor parameters (wavelength, system noise, slant range resolution), parameters related to the imaging geometry (interferometric baseline, local incidence angle), and target parameters. Volume scattering and temporal change (i.e. random motion of the scatterers, change of the scatterers) decrease the interferometric correlation. The system and geometry dependent effects are pretty well understood

and can be controlled by appropriate interferometric processing, as long as the system parameters are within a certain interval. The baseline dependence of the interferometric correlation, for example, may be eliminated in many cases by common spectral band filtering of the range spectrum. The estimation of the interferometric correlation requires a sufficient number of looks. As a compromise between maintaining a high spatial resolution and accurate estimation, an estimator with adaptive estimator window size was used.

In order to reduce speckle effects and obtain a backscatter intensity estimate at the pixel level which is representative for the ensemble average of the area around that pixel, the two registered SAR images of the interferometric pair are averaged. Minimum Mean Square Error filtering, as described by Frost et al. (1982), was then applied to the averaged image. Typically, the filter was applied to areas of 7x7 pixels of a 5-look image (5 azimuth looks).

The backscatter intensity change between the two images of the interferometric pair is defined as the absolute value of the ratio between the two images expressed in the logarithmic dB scale

$$\text{change[dB]} = \left| 10 \cdot \log \frac{\langle i_2 \rangle}{\langle i_1 \rangle} \right| \quad (1)$$

The brackets  $\langle \rangle$  stand for the ensemble average. Due to the speckle of the individual images it is essential to average sufficiently before the calculation of the ratio.

Finally, the texture of the backscatter image is defined as the ratio between the standard deviation and the average

$$\text{texture} = \frac{\langle \text{stdev}(i_1) \rangle}{\langle i_1 \rangle} \quad (2)$$

Again, the estimation of the ensemble averages requires sufficiently large estimator windows. It turns out that extremely strong scatterers in an image have the unwanted effect that high texture is obtained over an area corresponding to the entire size of the estimator window. This effect can be avoided to some degree if the texture estimation is followed by filtering with a moving average filter of larger size than the texture estimator.

## Forest Mapping Classification Algorithm

Based on the interferometric signatures a simple landuse classification algorithm was developed. A hierarchical decision tree algorithm using the criteria listed in Table 1 was used to generate a landuse map. In order to account for the specific conditions under which the data was acquired the classification scheme was slightly adapted. Forest was mapped based on its low interferometric correlation, low backscatter change between the two image of the interferometric pair, and backscattering intensities around -10 dB. While forest and agricultural fields are difficult to distinguish in the backscatter image this is less difficult using the interferometric correlation. Water and forest, on the other hand, show both low interferometric correlation due to motion of the scatterers. Therefore, these categories are easier distinguished in the backscatter image.

*Table 1. Decision rules of landuse classification algorithm. The criteria are applied hierarchically, in the order as listed. The value ranges used are indicated for the interferometric correlation ( $\gamma$ ), the average backscatter intensity of the two images ( $\langle \sigma^0 \rangle$ ), the backscatter intensity change between the two images ( $\Delta \sigma^0$ ), and the texture of the first backscatter image.*

landuse class	$\gamma$	$\langle \sigma^0 \rangle$ [dB]	$\Delta \sigma^0$ [dB]	texture
urban	> 0.4	> -7.0	> 0.0	> 1.0
layover	< 0.2	> -2.0	< 2.0	
water	< 0.2	< -15.0	> 2.0	
geom. change	< 0.3		> 2.0	
dielectric change	> 0.3		> 2.0	
sparse vegetation	> 0.6		< 2.0	
med. vegetation	0.35-0.6		< 2.0	
<b>forest</b>	<b>&lt; 0.35</b>	<b>&lt; -2.0</b>	<b>&lt; 2.0</b>	

## Results

ERS-1 data acquired in November 1991 during 3-day repeat-orbits over a region around Bern (Switzerland) has previously been analyzed and used for forest mapping (Wegmüller and Werner, 1995b; Wegmüller et al., 1997a). Here, these earlier results will be used for comparison purposes in order to assess the quality of the classification results achieved with ERS-1/2 Tandem data. The landuse classification of the November 1991 data is shown in Figure 1. The result was validated with a conventional forest map. An accuracy for the forest/non-forest classification of around 90% was reported by Wegmüller et al. (1997a). The November 1991 data were nearly ideal for the presented application because of the relatively short 3-day acquisition time interval, the short 58 m

baseline, and the acquisition during the winter season when the forest can best be distinguished from agricultural fields because the fields are bare or only sparsely covered with vegetation.

The November 1991 data are compared with results achieved using Tandem data. The exact dates and baselines of the Tandem data are listed in Table 2. An RGB color composite of the interferometric correlation (red), the backscatter intensity (green), and the backscatter change (blue) for the November 1995 data is first shown in Figure 2. Forest appears in green because of the low interferometric correlation and backscattering change values and of the medium to high backscatter intensities. The landuse classification of the November 1995 Tandem data (Figure 3) confirm the expected usefulness of Tandem data for landuse classification. Unlike with 3-day repeat data the approach with Tandem data leads to reasonably good results during spring (e.g. Figure 4 for the April 1996 data) and summer (Figure 5 for the July 1995 data) period, too. The shorter acquisition time interval results in an increase of the interferometric correlation of fields with grass or crops, improving the potential to distinguish fields from forest. These examples allow to conclude that landuse classification based on interferometric signatures from ERS-1/2 Tandem data is feasible and has a high potential not only because of the quality of the results which may be achieved, but also because of the good spatial and temporal coverage with appropriate image pairs.

Table 2: Dates, baseline and time difference  $\Delta t$  for interferometric data pairs used at the test site Bern (Switzerland).

Tandem pair	Sensors	Dates	Baseline [m]	D t [days]
-	ERS-1 & ERS-1	24.11.91 & 27.11.91	58	3
1	ERS-1 & ERS-2	4.6.95 & 5.6.95	117	1
2	ERS-1 & ERS-2	9.7.95 & 10.7.95	27	1
3	ERS-1 & ERS-2	13.8.95 & 14.8.95	-46	1
4	ERS-1 & ERS-2	22.10.95 & 23.10.95	108	1
5	ERS-1 & ERS-2	26.11.95 & 27.11.95	138	1
6	ERS-1 & ERS-2	10.3.96 & 11.3.96	-9	1
7	ERS-1 & ERS-2	14.4.96 & 15.4.96	-93	1

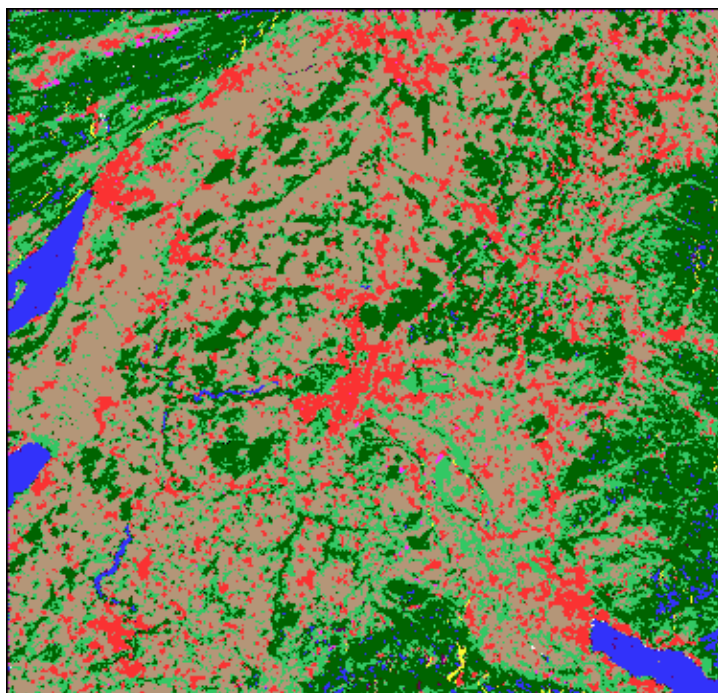


Figure 1. Landuse classification for the ERS-1 data of November 1991.

RGB color composite:

- Interferometric correlation
- Backscatter intensity
- Backscatter change

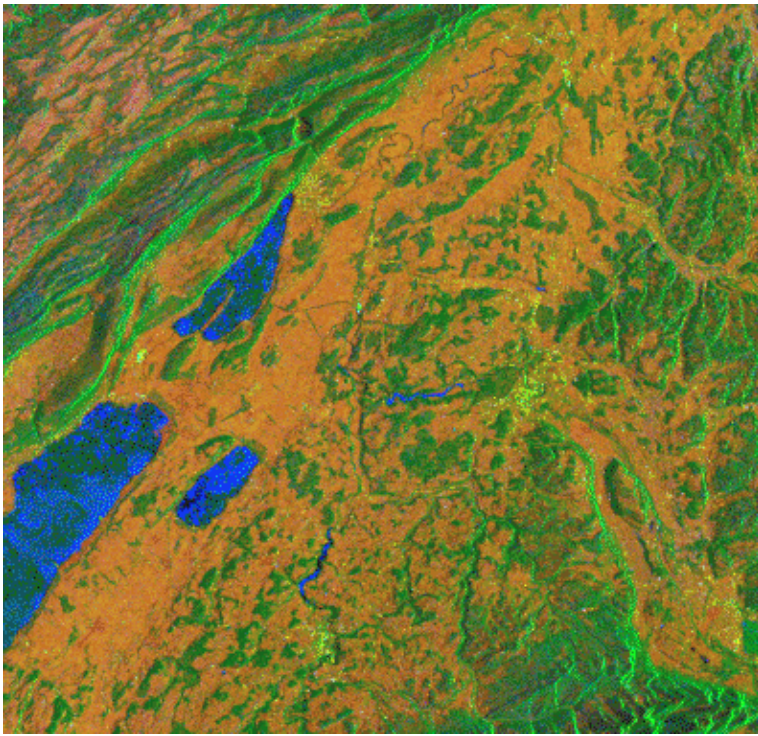
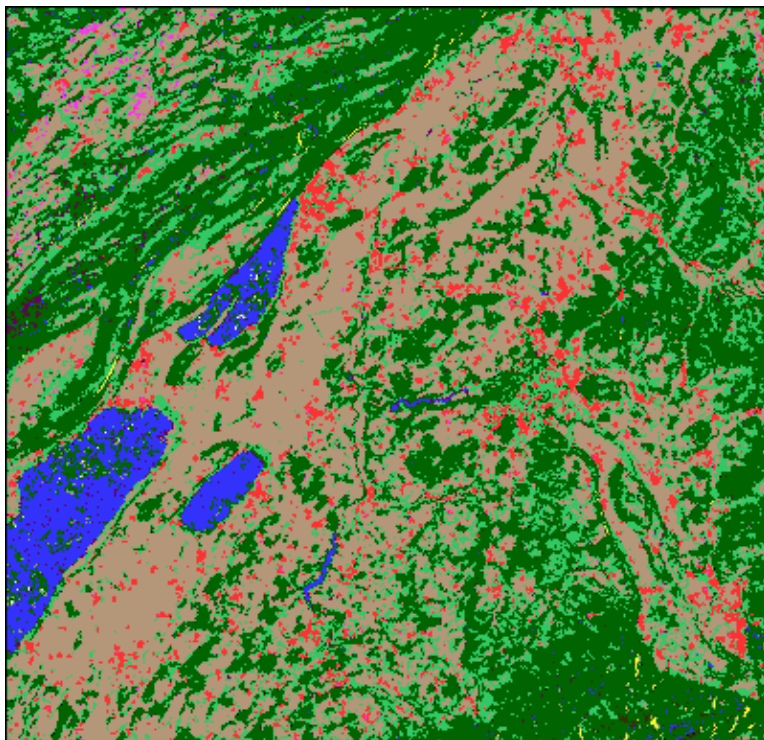


Figure 2. RGB color composite of the interferometric correlation (red), the backscatter intensity (green), and the backscatter change (blue) for the tandem pair 5 of November 1995.

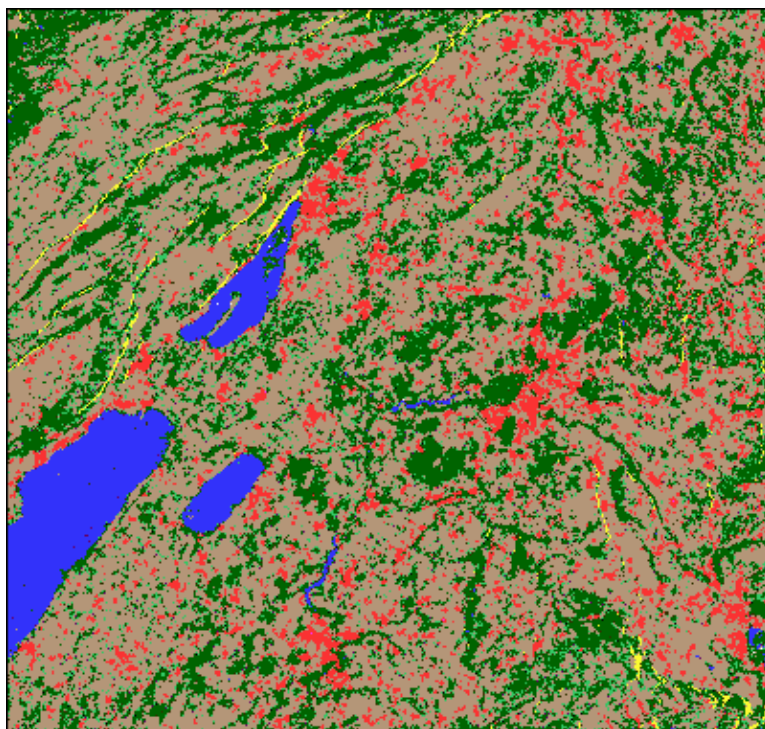


#### Color coding used:

- water
- urban area
- forest 1 (dense/coniferous)
- forest 2 (open/deciduous)
- sparse vegetation
- moisture change / freezing
- mechanical cultivation
- layover area

Figure 3. Landuse classification for tandem pair 5 of November 1995.

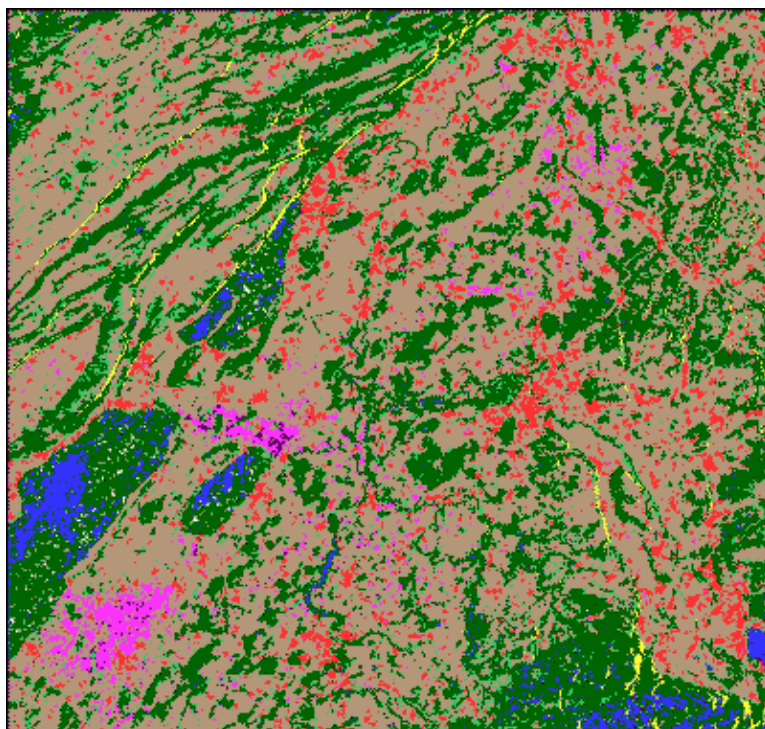




Color coding used:

- water
- urban area
- forest 1 (dense/coniferous)
- forest 2 (open/deciduous)
- sparse vegetation
- moisture change / freezing
- mechanical cultivation
- layover area

Figure 4. Landuse classification for the tandem pair 2 of July 1995.



Color coding used:

- water
- urban area
- forest 1 (dense/coniferous)
- forest 2 (open/deciduous)
- sparse vegetation
- moisture change / freezing
- mechanical cultivation
- layover area

Figure 5. Landuse classification for tandem pair 7 of April 1996.

## Validation

For the November 1991 data the results were validated with a conventional forest map. An accuracy for the forest/non-forest classification of around 90% was reported by Wegmüller et al. 1997a.

Based on the landuse inventory of the Federal Statistical Institute the forest mapping accuracy achieved with the Tandem data was validated. The classification algorithm applied was adapted only very slightly to the different data sets by modifying the coherence interval between the data sets acquired during periods with leaves on the deciduous trees (coherence interval 0.05 to 0.3) and times with no leaves on the deciduous trees (coherence interval 0.05 to 0.45). This adaptation was necessary in order to account for the seasonally changing coherence observed for deciduous forest stands and agricultural fields. Apart from that, the decision intervals remained identical (texture < 1.2, backscatter ratio interval 0.5 to 2.0, backscatter intensity interval 0.02 to 0.2). The confusion matrices are listed in Table 3. The very rugged areas of the Jura, Napf and the Alps were excluded from the validation analysis. For flat to hilly terrain an overall classification accuracy between 0.79 and 0.89 was found. These values are very satisfactory considering that the algorithm was not particularly tuned in order to achieve an optimum result. The high 0.79

classification accuracy found for the most critical data of July 1995 set is very promising. Based on a visual comparison of the RGB color composites, a classification accuracy higher than the 0.90 found previously for the November 1991 data may be expected for the more ideal data sets of the Tandem mission applying a tuned classification algorithm.

*Table 3: Forest mapping accuracy obtained with the various Tandem pairs over the Bern test site.*

Tandem pair	forest classif. as forest	forest classif. as non-forest	non-forest classif. as forest	non-forest classif. as non-forest	overall classif. accuracy
1	0.14	0.06	0.09	0.71	0.85
2	0.11	0.09	0.12	0.68	0.79
3	0.14	0.06	0.10	0.70	0.84
4	0.15	0.05	0.08	0.72	0.87
5	0.12	0.08	0.04	0.76	0.88
6	0.13	0.07	0.04	0.76	0.89
7	0.16	0.04	0.10	0.70	0.86

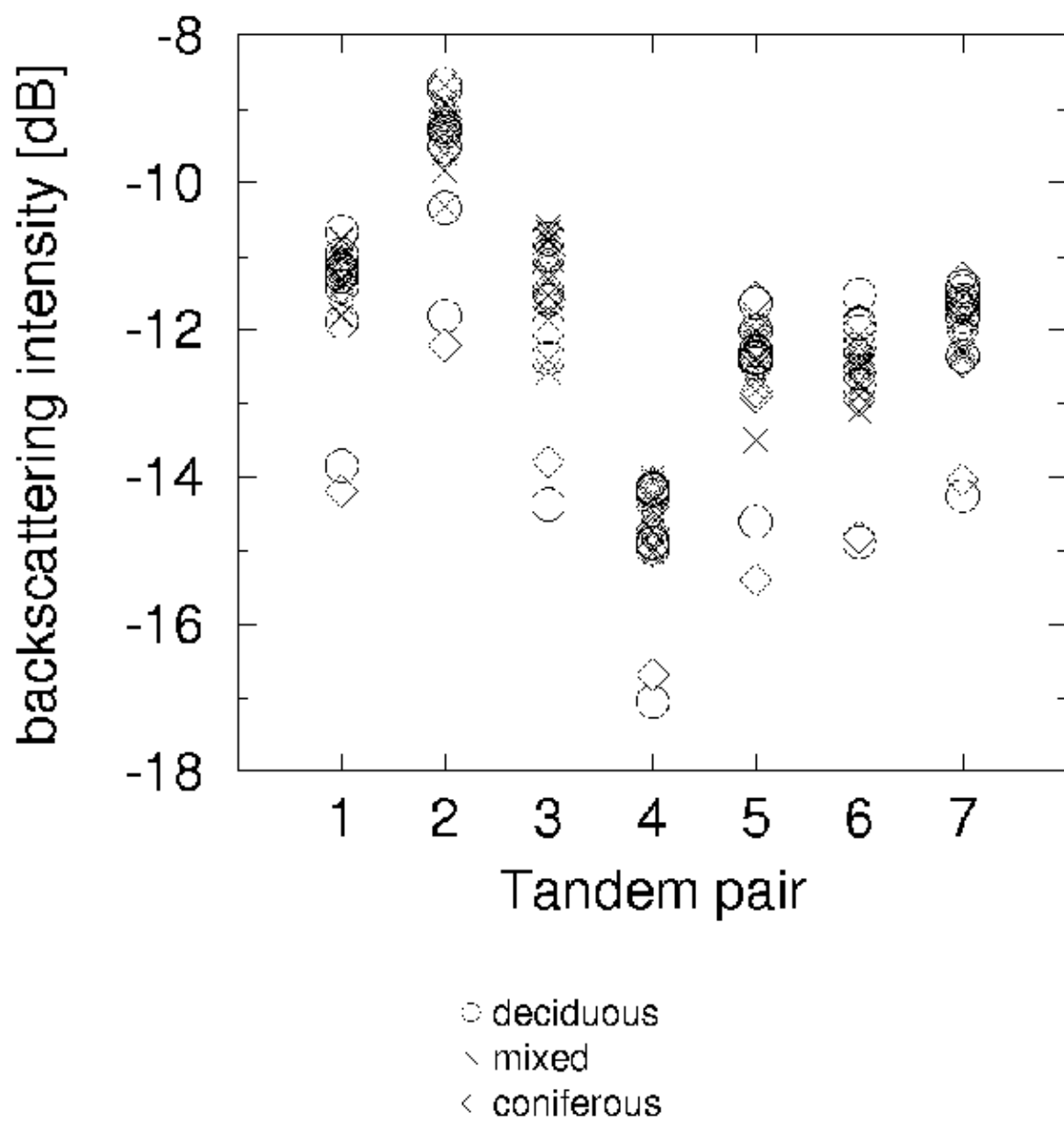
### Forest Type Discrimination Application Description

Based on ERS-1 data acquired during 3-day repeat orbits a certain potential of repeat-pass SAR interferometry for forest type discrimination was found. Previous studies (Wegmüller and Werner, 1995b) have shown indications that higher interferometric correlation is observed over deciduous forest than over coniferous forest for data acquired in winter, when the deciduous forests are without leaves. These findings were further investigated using the multi-seasonal interferometric data of the ERS-1/2 Tandem mission. For 26 known forest stands the interferometric signatures were extracted and related to the forest type. Three classes of forest type were distinguished, i.e. deciduous, mixed, and coniferous forest stands. The results for backscatter intensity, backscatter ratio, and interferometric correlation extracted from the 7 Tandem pairs listed in Table 1 are shown in Figures 6 to 8, respectively.

Notice that the extracted signatures are mean signatures for an entire forest stand and that the investigation was restricted to segmented data, i.e. it is assumed that a segmentation is performed before the signature analysis or classification. In the Bern test-site most forest stands are in fact very small and heterogeneous and therefore not ideal for this remote sensing investigation.

Before the interpretation of the interferometric signatures some comments on the radiometric calibration have to be made. The data were processed with our own SAR processor which includes radiometric calibration for the slant range distance and the antenna diagram. All filtering operations are designed in order to keep the image intensity unchanged. But in spite of that there is quite some uncertainty on the calibration of the data. First, we were informed by ESA on the data delivery that for the first two (or maybe three) ERS-2 data acquisitions something was different with the gain setting (commissioning phase). We tried to correct that but we do not know how well we succeeded. Second, the gains for ERS-1 and 2 are different. A comparison of the values of the Tandem pairs indicates that we did not use the best correction value. This also indicates that the difference may have changed. In conclusion, from the extracted ERS SAR backscatter intensities and ratios (Figures 6 and 7) we conclude that a separation of the observed coniferous and deciduous forest stands does not seem to be possible.

The extracted interferometric correlation values (Figure 8), on the other hand, confirm the previous observation of higher correlation for deciduous forest stands than for coniferous forest stands during winter season or more precisely during the time when the deciduous trees are without leaves (see e.g. Tandem pairs 4, 5, 6 and 7). For the summer season (e.g. Tandem pairs 1, 2 and 3) this difference is not observed, or at least much less pronounced, with low interferometric correlation for all forest stands in spite of the short one day acquisition time interval. Based on the data it may be concluded that the distinction of deciduous, mixed, and coniferous forest stands based on different levels of the interferometric correlation is promising during the time when the deciduous trees are without leaves, i.e. in winter.



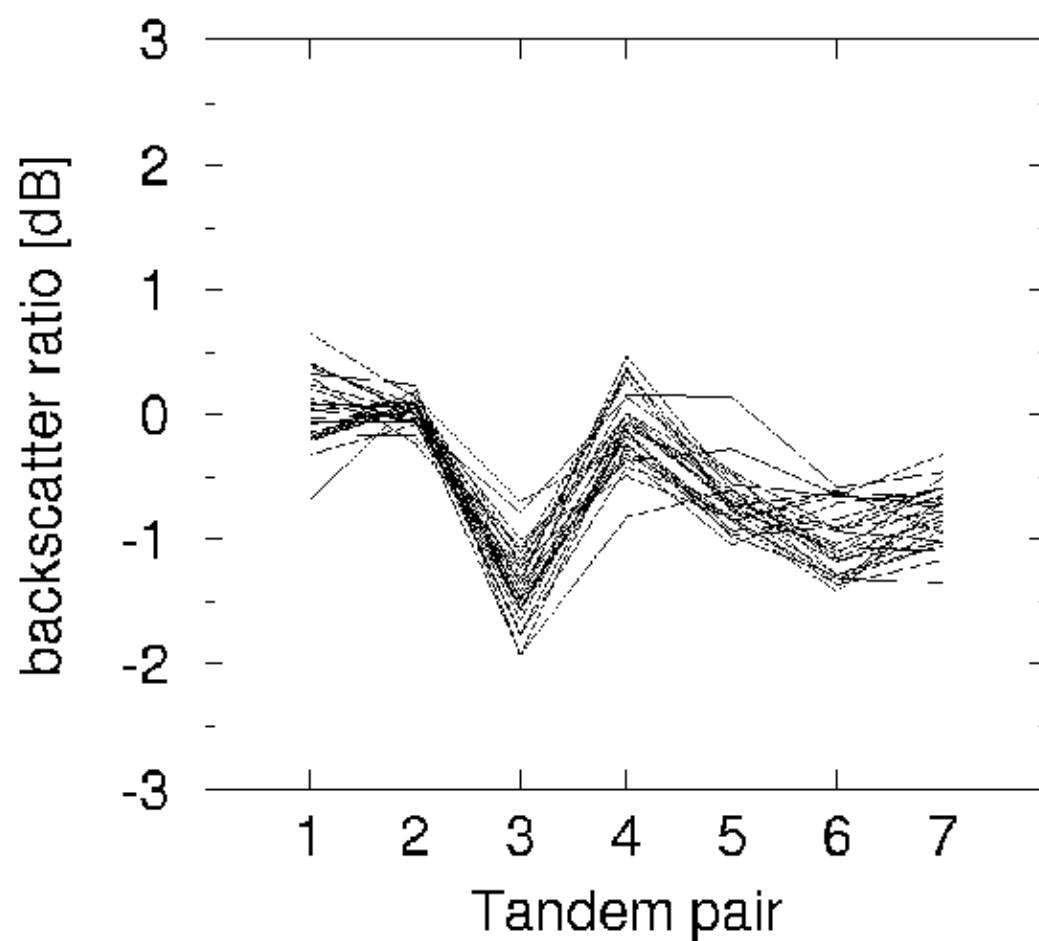
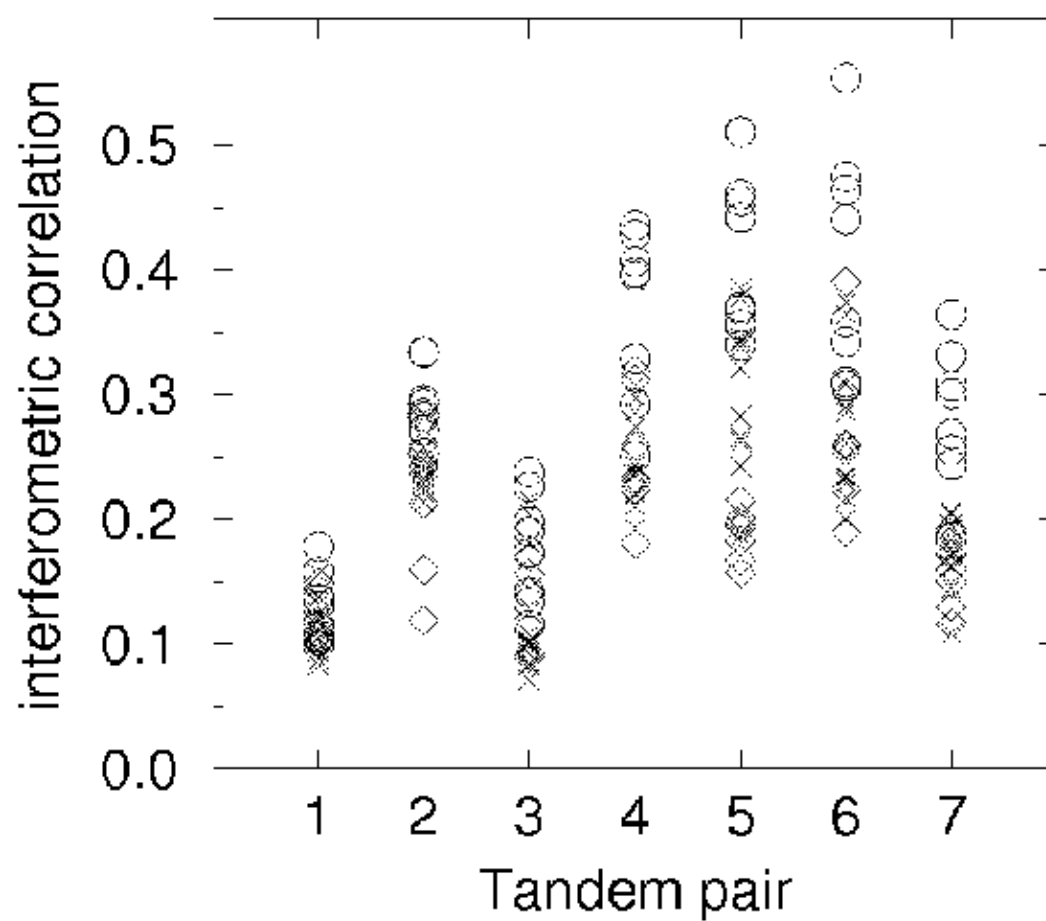


Figure 7. Ratio between ERS-1 and ERS-2 backscattering for forest stands versus Tandem pair.





○ deciduous  
 \ mixed  
 < coniferous

Figure 8: Coherence of forest stands for ERS-1/2 Tandem pairs.

## Algorithm Development and Validation

An algorithm was developed in order to classify different forest types. The forest types were distinguished based exclusively on the interferometric correlation, with the lowest interferometric correlation corresponding to coniferous forest, intermediate values to mixed forest and the highest values to deciduous forest. The exact thresholds used for the classification are listed in Table 4. The forest type discrimination results achieved with the winter Tandem pairs 4, 5, 6 and 7 for the selected 26 forest stands are listed in Table 4. A reliable separation for all three forest types, i.e. deciduous, mixed, and coniferous forest stands, was possible only with the November 1995 Tandem pair. For the other winter Tandem pairs only the two classes deciduous forest versus mixed and coniferous forest were distinguished.

The achieved accuracy for the segmented data, i.e. for the test forest stands, is quite high. This is only true for the segmented data, a pixel based application of the classification with the same thresholds would lead to a much lower classification accuracy. Because of the influence of the interferometric baseline, meteorological conditions (affecting the motion of the trees), and the acquisition time interval, we did not try to develop a generally applicable forest type discrimination algorithm.

Table 4. Thresholds used for the classification of coniferous, mixed and deciduous forest, and overall classification accuracy.

Tandem Pair	Forest types classified	Coherence thresholds used	Overall classification accuracy
4	deciduous coniferous & mixed	> 0.32 < 0.32	0.92
5	deciduous mixed coniferous	> 0.35 0.22 - 0.35 < 0.22	0.85
6	deciduous coniferous & mixed	> 0.32 < 0.32	0.81
7	deciduous coniferous & mixed	> 0.23 < 0.23	0.96

## Conclusions

Based on the geometric information contained in the interferometric phase, on the interferometric correlation, on the two backscatter intensities of an interferometric pair, and on the texture of the backscatter image, forest maps for a part of Switzerland were generated. The maps were validated against available landuse inventory. ERS-1/2 Tandem data acquired during different seasons were analyzed. As a result of the short one day acquisition interval as compared to the 3 and more days with ERS-1 data only, the approach with Tandem data was applicable also during spring, summer and fall. During the winter season the most accurate results were obtained, because the forest can be best distinguished against agricultural fields, being the fields bare or only sparsely covered with vegetation. The distinction of deciduous, mixed, and coniferous forest stands based on different levels of the interferometric correlation for the Bern test-site was found to be promising during winter time using segmented data.

The classification algorithm used here was very general in order to allow adaptation to different test-sites, classes, seasons, and input data-sets. The key of the classification algorithm was a table with a list of lower and upper thresholds for each class and input parameter. In future work, the forest mapping and forest type discrimination algorithms should be applied to other test-sites. Boreal and tropical forest, for instance, as poorly mapped and difficult to access test-sites, represent very important ecosystems to be studied.

## Acknowledgments

This work was supported by ESA ESTEC under ESA/Contract 11740/95/NL/PB(SC) and by the Swiss Federal Office for Education and Science. ERS-1/2 raw data were provided under ESA-A02.JRC101. The Swiss Federal Statistical Institute is acknowledged for providing the digital landuse map "Arealstatistik".

## References

- Frost V.S., Stiles J.A., Shanmugan K.S., Holtzman J.C., 1982:  
 A model for radar images and its application to adaptive digital filtering of multiplicative noise. *IEEE Trans. Pattern Analysis and Machine Intelligence*, 4(2), 157-165.
- Wegmüller U., Werner C.L., Nuesch D., Borgeaud M., 1995a:  
 Land-surface analysis using ERS-1 SAR interferometry. *ESA Bulletin*, 81, 30-37.
- Wegmüller U., Werner C. L., 1995b:  
 SAR interferometric signatures of forest, *IEEE Geosci. Remote Sensing*, 33(5), 1153-1161.
- Wegmüller U., Werner C. L., 1996:  
 Land applications using ERS-1/2 Tandem data. *FRINGE 96: ESA Workshop on Applications of ERS SAR Interferometry*. 30 September to 2 October, Remote Sensing Laboratories, University of Zurich, Switzerland.

Wegmüller U., Werner C.L., 1997a:  
Retrieval of vegetation parameters with SAR interferometry. *IEEE Geosci. Remote Sensing*, 35(1), 18-24.

Wegmüller U., Werner C. L., 1997b:  
Gamma SAR Processor and Interferometry Software. *3rd ERS Symposium*, Florence, 18-21 March.